PaleoBios 37:1–14, February 5, 2020

PaleoBios

OFFICIAL PUBLICATION OF THE UNIVERSITY OF CALIFORNIA MUSEUM OF PALEONTOLOGY

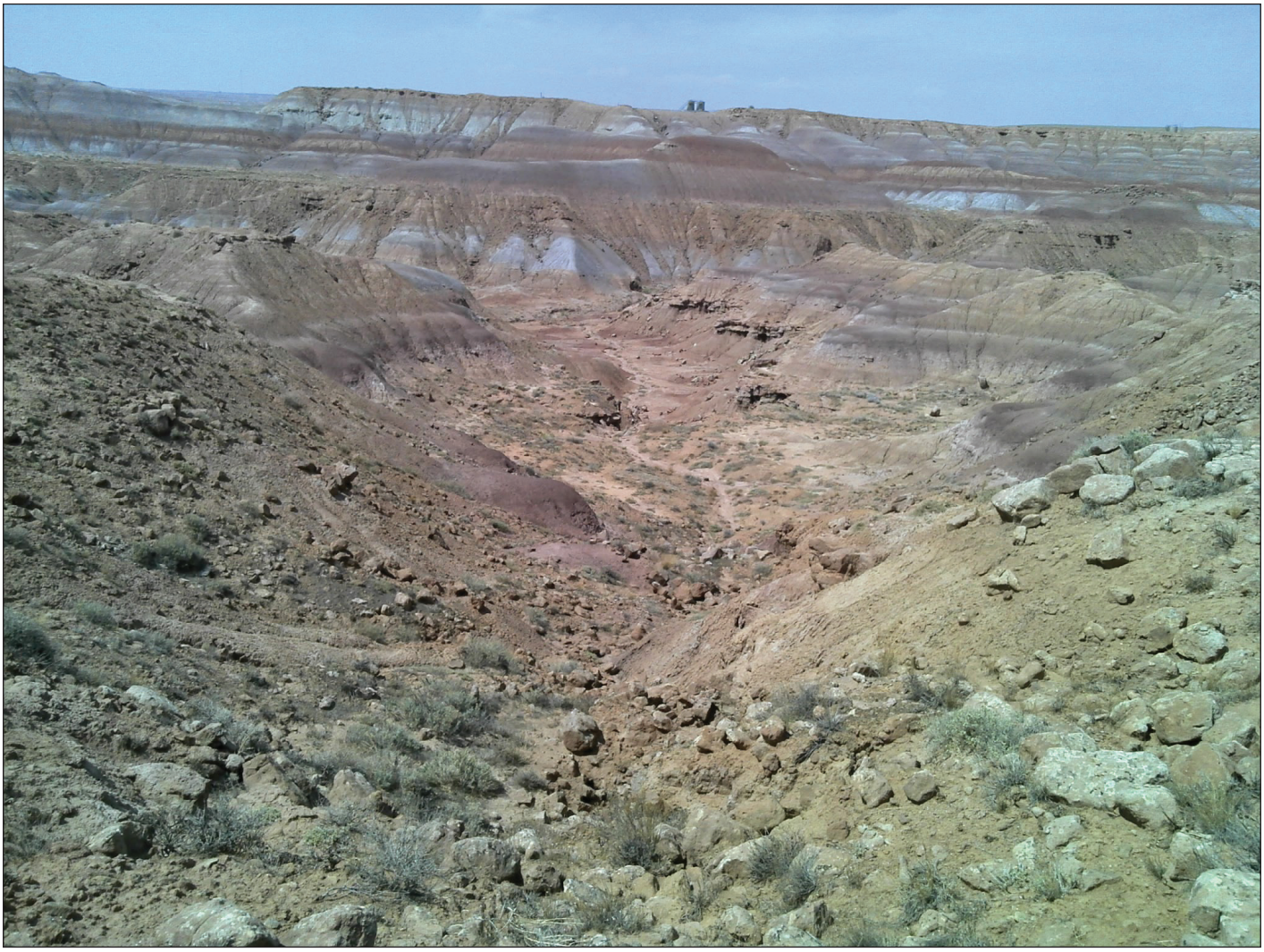

HEATHER F. SMITH, DANIEL JAGER, J. HOWARD HUTCHISON, BRENT ADRIAN & K.E. BETH TOWNSEND (2020). Epiplastral and geographic variation in *Echmatemys*, a geoemydid turtle from the Eocene of North America: A multi-tiered analysis of epiplastral shape complexity.

Cover: View of the Uinta Basin, Utah, site where the *Echmatemys uintensis* and *E. callopyge* specimens were discovered.
Citation: Smith, H.F., D. Jager, J.H. Hutchison, B. Adrian, and K.E.B. Townsend. 2020. Epiplastral and geographic variation in *Echmatemys*, a geoemydid turtle from the Eocene of North America: A multi-tiered analysis of epiplastral shape complexity. *PaleoBios*, 37. ucmp_paleobios_46852.

Epiplastral and geographic variation in *Echmatemys*, a geoemydid turtle from the Eocene of North America: A multi-tiered analysis of epiplastral shape complexity

HEATHER F. SMITH[1,2*], DANIEL JAGER[1], J. HOWARD HUTCHISON[3], BRENT ADRIAN[1], and K. E. BETH TOWNSEND[1]

[1]Department of Anatomy, Midwestern University, 19555 N. 59th Avenue, Glendale, Arizona 85308, USA; *hsmith@midwestern.edu*; *jagerd61@gmail.com; badria@midwestern.edu; btowns@midwestern.edu*
[2]School of Human Evolution and Social Change, Arizona State University, P.O. Box 2402, Tempe, Arizona 85287, USA.
[3]University of California Museum of Paleontology, University of California Berkeley, 1101 Valley Life Sciences Building, Berkeley, California 94720, USA; *howard.hutchison@gmail.com*

Numerous geoemydid turtle fossils from the extinct genus *Echmatemys* have been recovered from the middle Eocene Uinta Formation, Uinta Basin, Utah over the past several decades. Here, we tested whether co-occurring Uintan species *Echmatemys callopyge* and *E. uintensis* can be reliably differentiated based on epiplastral morphology, and whether their geospatial distributions overlapped significantly. The geographic spatial and stratigraphic distributions of Uinta Basin *E. callopyge* and *E. uintensis* specimens were compared using ArcGIS and analysis of variance (ANOVA). The analysis revealed overlapping geographic distributions of these two species, and no significant differences in stratigraphic dispersal. This finding of extensive geospatial overlap between the two Uintan *Echmatemys* species highlights the need for accurate taxonomic identification, such as the gular scale morphology validated here. In addition, we sought to address a methodological question regarding the relative efficacy of data complexity in this context. Using epiplastra from three additional Eocene species of *Echmatemys*, we employed hierarchical analyses of increasing data complexity, from standard linear dimensions to 2D geometric morphometrics to 3D laser scans, to determine the degree to which data complexity contributes to taxonomic assessments within this genus. Uintan species *E. callopyge* and *E. uintensis* were found to differ significantly in epiplastral shape as captured by all three categories of data. These findings verify that these two co-occurring species can be differentiated consistently using the shape of the gular scale, and that the use of geometric morphometrics can improve identification of fragmentary specimens. Among the non-Uintan species, dorsal and ventral 2D landmark data reliably differentiated among species, but the linear dimensions were less useful.

Keywords: ArcGIS, geometric morphometrics, Uintan NALMA, turtle evolution, Geoemydidae

INTRODUCTION

The collection and classification of fossil geoemydid turtle specimens from North America began in the late 19th century (Hay 1906, 1908, Gilmore 1915). Since then, collection efforts have resulted in a large number of specimens from the Eocene deposits of the Rocky Mountains. The geoemydid *Echmatemys* Hay (1906), was an abundant genus consisting of numerous species, all of which were large-bodied with a robust shell. Although a large number of specimens have been collected, they are often incomplete and damaged. While shell fragments may be in poor condition, it is still possible to extract information on taxonomy and geographic distribution.

Since its initial description, the number of recognized species within *Echmatemys* has varied widely (e.g., Hay 1906, 1908, Gilmore 1915, Roberts 1962, Vlachos 2017). Hay (1908) described thirteen different *Echmatemys* species, plus two additional species that he designated "?*Echmatemys,*" Gilmore (1915) named several additional species, *Echmatemys depressa*, *E. douglassi*, *E. hollandi*, and *E. obscura*, based primarily on minor differences in scale patterns. However, a subsequent reassessment by Roberts (1962) combined many of those originally described into just four species: *E. douglassi*, *E. septaria* Cope (1873a), *E. uintensis* Hay (1908), and another unnamed species (likely the later-named genus *Bridgeremys*

*author for correspondence

Citation: Smith, H.F., D. Jager, J.H. Hutchison, B. Adrian, and K.E.B. Townsend. 2020. Epiplastral and geographic variation in *Echmatemys*, a geoemydid turtle from the Eocene of North America: A multi-tiered analysis of epiplastral shape complexity. *PaleoBios*, 37. ucmp_paleobios_46852.
Permalink: https://escholarship.org/uc/item/9cn4w7n6

Hutchison, 2006). In particular, Roberts (1962) subsumed *E. hollandi*, *E. obscura*, and *E. callopyge* Hay (1908) into *E. septaria*. Subsequently, Vlachos (2017) considered *E. uintensis* to be a junior synonym of *E. wyomingensis*.

The Uinta Formation, Uinta Basin, Utah is a key site for *Echmatemys* fossils, in which specimens of this genus are extremely common. More than a century ago, Hay (1908) described from the Uinta Formation two species, *E. callopyge* and *E. uintensis*. These two species differed in body size (Hay 1908, Gilmore 1915, Roberts 1962), and may have occupied different ecological niches. Further, morphological differences in the anterior plastral lobe and first vertebral scale are key traits differentiating the two species (Hay 1908). Specifically, the epiplastron of *E. callopyge* was particularly narrow. Since then, the shape and size of the epiplastral lip were used by several researchers to separate these taxa (Gilmore 1915, Roberts 1962, Hutchison 2002). In particular, Hutchison (2002) noted that the gular scale in *E. uintensis* is wider and shorter compared to the elongated, narrow gular scale of *E. callopyge*. Vlachos (2017) noted that the gular scales of *E. callopyge* continue onto the entoplastron, unlike some other species of *Echmatemys*. Despite the abundance of *Echmatemys* specimens from the middle Eocene of the Western Interior, many are fragmentary, rendering species-level identifications challenging. Thus, the validation of diagnostic characters that can distinguish between fragmentary specimens is crucial.

Morphology of the epiplastron has been demonstrated by previous studies to distinguish among various testudine taxa. Epiplastral morphology has been applied to species-level identifications in numerous turtle clades, including basal Mesozoic turtles (Joyce 2017), Trionychidae Gray, 1825 (Vitek and Joyce 2015), Chelydridae Gray, 1831 (Joyce 2016), Bothremydidae Baur, 1891 (Gaffney et al. 2006), Pan-testudinoidea Joyce et al., 2004 (Vlachos 2017), and Thalassochelydia Anquetin et al. (2017). A dorsal epiplastral process has also been described in many primitive turtles (reviewed in Joyce et al. 2006). Additionally, the relative size of the gular scales and their relationship to the extragular scales is a key character used to differentiate among species of Baenidae Cope, 1873b (e.g., Brinkman 2003, Lyson and Joyce 2010, Joyce and Lyson 2015, Adrian et al. 2019).

Despite the fact that numerous *E. callopyge* and *E. uintensis* specimens were recovered from the Uinta Formation, the geotemporal distribution of the genus in the Uinta Basin is not known. Thus, it is currently unclear whether the two species experienced extensive geospatial overlap, and if so, whether they occupied separate ecological niche spaces. Other biotic factors, such as differences in body size between the two species, may have influenced how they partitioned the available ecospace. If the species exhibited significant geospatial overlap, then development of accurate methods for identifying fragmentary fossil remains would be crucial. Here, we sought to evaluate the geospatial distribution of co-occurring *E. callopyge* and *E. uintensis* in the Uinta Basin, and to test the applicability of 3D and 2D morphometric techniques to differentiate between their epiplastral shapes (Figs. 1, 3). Finally, we expanded this comparison to other species of *Echmatemys* from the early and middle Eocene of the Western Interior, including *E. haydeni* and *E. septaria* (Bridgerian) and *E. testudinea* (Wasatchian).

MATERIALS AND METHODS

Geospatial analyses were conducted to evaluate the geographic and stratigraphic associations of *Echmatemys* specimens in the Uinta Basin. Multi-tiered analyses were then conducted in order to quantify morphological variation in the epiplastron of Eocene geoemydid *Echmatemys*, and determine whether this variability is taxonomically informative. The shape of the entire gular scale was quantified and compared at various levels of data complexity. In particular, we analyzed the following hierarchy of increasing data density: 1) standard linear dimensions; 2) 2D landmark and semilandmark data; and 3) 3D laser scans of complete epiplastra. In addition, one goal of this study was to determine whether data complexity provided additional taxonomically informative data in this context. Thus, the results from each analytical step were compared to assess the consistency of results from the various tiers of the analysis.

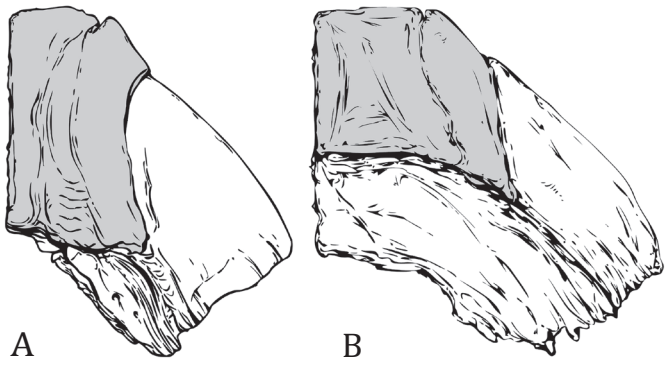

Figure 1. Morphological differences in dorsal epiplastral shape between Uintan *Echmatemys* species. **A**. *Echmatemys callopyge* (UMNH.VP.27220). **B**. *Echmatemys uintensis* (UMNH.VP.26558). The gular scale is indicated in grey.

Geological Setting

The Uinta Basin study site considered here is bounded by the Green and White Rivers, and lies between latitudes 40°00' and 40°30' north and longitudes 109°00' and 109°45' west (Townsend et al. 2006). The section extends 366 meters through the older lithostratigraphic unit, Uinta B (0–137 m), to the younger Uinta C (140–366 m) (Townsend et al. 2006). Stratotypes for biochrons Ui2 and Ui3 (Gunnell et al. 2009) occur in the Uinta Basin, and the localities from which the *Echmatemys* fossils were recovered fall within these stratotype sections (Gunnell et al. 2009, Townsend et al. 2006, 2010).

Specimens and Institutional Abbreviations

The specimens examined in this study are from the following collections: **AMNH**, American Museum of Natural History, New York, New York; **BYU**, Brigham Young University Paleontology Museum, Provo, Utah; **UCMP**, University of California Museum of Paleontology, Berkeley, California; **UFH**, Utah Field House of Natural History State Park, Vernal, Utah; **UMNH**, Natural History Museum of Utah, Salt Lake City, Utah (Table 1).

We included specimens from five Eocene chronospecies of *Echmatemys* (Table 1): *E. testudinea* from the early Eocene, Wasatchian North American Land Mammal Age (NALMA) (55.4–50.3 Ma); *E. haydeni, E. septaria,* and *E.* "Spider Creek" from the early middle Eocene, Bridgerian NALMA (50.3–46.2 Ma); and *E. callopyge* and *E. uintensis* (e.g., Hay 1908, Gilmore 1915, Prothero 1996) from the middle to late middle Eocene, Uintan NALMA (46.2–42.0 Ma). In addition, the holotypes of *E. uintensis* (AMNH FR 19403) and *E. callopyge* (AMNH FR 2087) were included for comparison. However, the type specimens of *E. septaria*, *E. haydeni*, and *E. testudinea*, lack complete epiplastra and therefore could not be included.

Supplementary Material table 1 (SM 1) is a complete list of specimens included in the comparative 2D analysis. Supplementary Material table 2 (SM 2) is the raw data file of 3D coordinates from the 3D epiplastral analyses.

Data Collection

Geographic data—Specific geographic provenance information in the form of UTM coordinates and relative meter depth of locality were entered into ArcGIS 10.3.1 (Environmental Systems Research Institute (ESRI 2011) for all Uintan *E. uintensis* and *E. callopyge* specimens. Information on geographic easting and northing, locality, and stratigraphic depth (meter level) for each specimen were also recorded and entered into SPSS 22 (IBM Corp. 2013).

Table 1. *Echmatemys* taxa included in the present study, including sample sizes, temporal context, and museum collections. Abbreviations: **NALMA**=North American Land Mammal Age, see Materials and Methods for institutional abbreviations.

Taxon	Sample Size	NALMA	Epoch	Museum Collection(s)
E. testudinea	13	Wasatchian	Early Eocene	UCMP
E. haydeni	11	Bridgerian	Early Middle Eocene	UCMP
E. septaria	26	Bridgerian	Early Middle Eocene	UCMP
E. "Spider Creek"	19	Bridgerian	Early Middle Eocene	UCMP
E. callopyge	16	Uintan	Middle to Late Middle Eocene	BYU, UMNH, UCMP, UFH
E. uintensis	21	Uintan	Middle to Late Middle Eocene	BYU, UMNH, UCMP, UFH
Total	**115**			

Morphological data—In keeping with the multi-tiered nature of this study, morphological data collection proceeded in a hierarchical manner:

1) Traditional linear dimensions captured the relative length and width of the gular scale (Fig. 2), measured digitally from high resolution photographs using tpsDig2 v2.22 (Rohlf 2006). Two particular variables were obtained: (1) distance from the epiplastral tooth to the anatomical midline, measured on a line perpendicular to the midline (Tooth-Midline =TM) and (2) distance from the epiplastral tooth to the inferior lip of the gular-humeral sulcus (Tooth-Lip=TL) (Fig. 2A). A variable indicating the relative width of the gular scale was then calculated using a ratio of TM/TL. Photos included were taken at high resolution. Photographic measurements were selected over handheld caliper measurements, because the data collection was more efficient. Due to the high resolution of the photographs, any differences between digital and manual caliper measurements are likely to be slight.

2) Two-dimensional landmarks (n=4) and 30 equally-spaced semilandmarks on each of the dorsal and ventral surfaces of the epiplastron were digitized from high resolution photographs using tpsDig2 2.22 (Fig. 2B). Coordinates of the landmarks and semi-

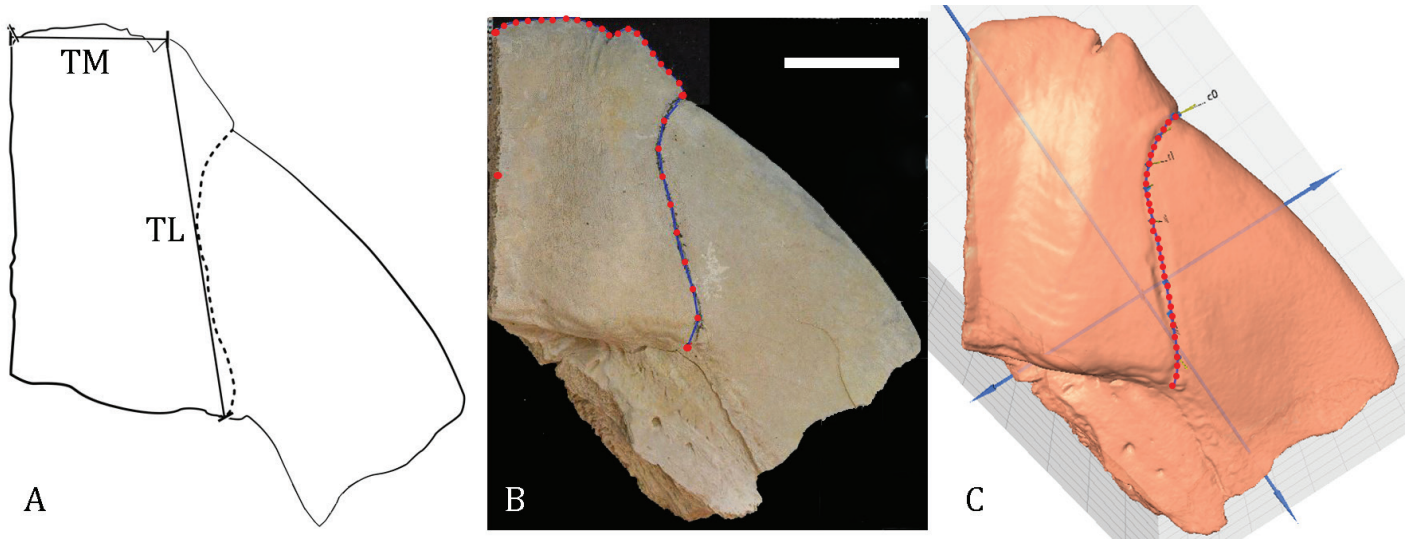

Figure 2. A. Standard linear measurements for quantifying the dimensions of the gular scale on the epiplastron of *Echmatemys* species depicted on UMNH.VP.27220. TM=tooth-midline: Distance between the epiplastral tooth and the anatomical midline. TL=tooth-lip: Distance between the epiplastral tooth and the caudal lip of the gular-humeral sulcus. **B.** Two-dimensional epiplastral landmarks and semilandmarks used in 2D geometric morphometric comparisons of this study: Ventral surface. Data points were digitized from digital photographs. **C.** Three-dimensional epiplastral landmarks and semilandmarks used in 3D geometric morphometric analyses in this study. All data points were obtained from 3D NextEngine laser scans. Scale bar=2 cm.

landmarks were extracted using tpsUlt 1.70 x64 (Rohlf 2006), and the 2D coordinate data were imported into MorphoJ v.1.06d (Klingenberg 2011) for subsequent geometric morphometric analyses. Equidistant semilandmarks were employed because they retained the most accurate landmark order and separated species along PC1. Sliding semilandmark methods (Minimum Bending Energy, Procrustes Distance) were attempted but not reported due to landmarks exceeding the cranial edge of the epiplastra. An intraobserver error analysis indicated no significant error in landmark placements between trials.

3) Three-dimensional scans of complete epiplastra were generated using a NextEngine 3D scanner. In NextEngine ScanStudio, lower resolution (.ply format) files were polished and exported to increase the visibility of the sulci. Using Landmark 3.6d (Institute for Data Analysis and Visualization), approximately 100–200 points were digitized manually along each of the dorsal and ventral surfaces of the gular-humeral sulcus (Fig. 2C). This set was reduced to 30 semilandmarks with ChainMan3D (Sheets IMP), and the 3D coordinate data imported into MorphoJ v.1.06d (Klingenberg 2011) for subsequent geometric morphometric analyses (SM 2). The dataset was divided into dorsal, ventral, and full epiplastral landmarks.

Analytical Methods

Geographic data—We used geographic information systems (GIS) to compare spatial and temporal distributions of Uintan *E. callopyge* and *E. uintensis* in ArcGIS 10.3.1 (ESRI 2011). The coordinates were projected within ArcGIS using the datum WGS 1984 12N projection. Natural breaks (Jenks) were identified using Jenks Natural Breaks Classification (Jenks 1967), which allowed classification of stratigraphically similar groups within the 366-meter section and generate relative symbol sizes. Natural breaks are categories based on natural clusters in the data, and are appropriate in geographic analyses in which there are relatively large jumps in data values (Jenks 1967). Five natural breaks were identified: 25–58 m, 59–99 m, 100–140 m, 141–256 m and 257–366 m. An imagery base map within ArcGIS was overlaid to compare the geographic and stratigraphic ranges of specimens. Using SPSS 22 (IBM Corp. 2013), an ANOVA (analysis of variance) was conducted to determine whether significant differences existed between species in geographic easting or geographic northing, or stratigraphic meter level within the section. An assessment of locality associations was also conducted.

In order to compare the geographic dispersion patterns of fossil and extant Geoemydidae, distribution data for modern taxa were downloaded from the iDigBio database (https://www.idigbio.org, accessed December 7, 2016). This step enabled us to assess overlapping geographic distributions in extant geoemydid species.

Instances of multiple congeneric species occupying the same geographic area were noted.

Morphological data—In keeping with the multi-tiered nature of this study, morphological data analysis proceeded in a hierarchical manner:

1) Traditional linear dimensions: An ANOVA was conducted to determine whether significant differences existed in the sample for all three linear variables: tooth to midline (TM), tooth to caudal lip of gular scale margin (TL), and the ratio of tooth-midline/tooth-lip (TM/TL) (Fig. 2). Tukey post hoc tests determined whether significant pairwise differences existed between each pair of taxa for these variables. A Regression Analysis assessed the relationship between variables TM and TL in each species, and determined whether the correlations differed significantly among species. Finally, another Regression Analysis assessed the relationship between the TM/TL ratio and the first principal component (PC1) from the Principal Components Analysis (PCA) from the 2D landmark data. This analysis enabled an assessment of the comparability of the two types of 2D data. All linear data analyses used SPSS 22 (IBM Corp. 2013).

2) Two-dimensional landmarks: In MorphoJ v.1.06d, 2D landmark data were first aligned using a Generalized Procrustes Analysis, in which specimens are scaled, rotated, and translated using a least squares fitting algorithm (Gower 1975, Goodall 1991, Dryden and Mardia 1998). A PCA was used to graph the distribution of epiplastral shape among chronospecies. A Procrustes ANOVA assessed whether significant differences existed in 2D epiplastral shape among taxa in the sample. Finally, to determine whether chronospecies differed significantly in morphospace, the Procrustes rotated coordinates (i.e., Procrustes residuals) were used to calculate a matrix of Procrustes distances (*D*) among taxa for the dorsal and ventral epiplastral landmark sets. A permutation test with 10,000 replicates assessed the significance of the pairwise distances between taxa, and a Bonferroni correction for multiple tests was applied. As a comparison with the results from the traditional linear dimensions, individual specimen scores for PC1 were compared to the TM/TL ratio using a Regression Analysis.

3) Three-dimensional landmarks: Using MorphoJ v.1.06d, the 3D landmark datasets were each superimposed using a Generalized Procrustes Analysis (Gower 1975, Goodall 1991, Dryden and Mardia 1998). PCAs were conducted and the first several principal components plotted to assess overall shape variation in the sample. In order to visualize morphological differences between species, a shape exploration determined how the taxa varied along each of the major PCs. Specimens were then warped along PC1 to demonstrate their major shape differences using morphologika2 v2.5 (O'Higgins and Jones 2006). Procrustes distances (*D*) were calculated between *E. callopyge* and *E. uintensis*, and *p*-values were generated using permutation tests as described above to determine whether significant differences in 3D epiplastral shape existed between these co-occurring species. We applied a Bonferroni correction for multiple comparisons.

RESULTS

Geospatial Data

Echmatemys—ArcGIS revealed overlapping geographic distributions for Uinta Basin *E. callopyge* and *E. uintensis* (Fig. 3). Specimens of both species were found clustered together in certain areas across the study site (Fig. 3; Table 2). An ANOVA also revealed no significant differences between *E. callopyge* and *E. uintensis* in geographic easting (F=1.582, p=0.216) or northing values (F=0.001, p=0.997).

In addition, there was no statistically significant difference in the stratigraphic depth (meter levels) in the section from which each species was recovered (F=0.260, p=0.613). Specimens from both species were found from low in the section (25 m) to the uppermost section at the contact with the Duchesne River Formation (366 m). There was also extensive overlap in localities between the two species. Of the thirteen localities from which *E. callopyge* was recovered, *E. uintensis* was also found in six of these. Therefore, *E. callopyge* and *E. uintensis* exhibited extensive spatial overlap in the Uinta Basin, both in geographic location and depth within the section.

Extant geoemydids—The comparison of extant geoemydid distributions indicated that in several modern geoemydid genera, congeneric species may inhabit overlapping geographic distributions. Specifically, within the genus *Rhinoclemmys* Fitzinger, 1835 (Neotropical wood turtles), *Rhinoclemmys annulata* Gray (1860), *R. areolata* Duméril et al. (1851), *R. funerea* Cope (1876), *R. pulcherrima* Gray (1856) and *R. punctularia* Daudin (1801)

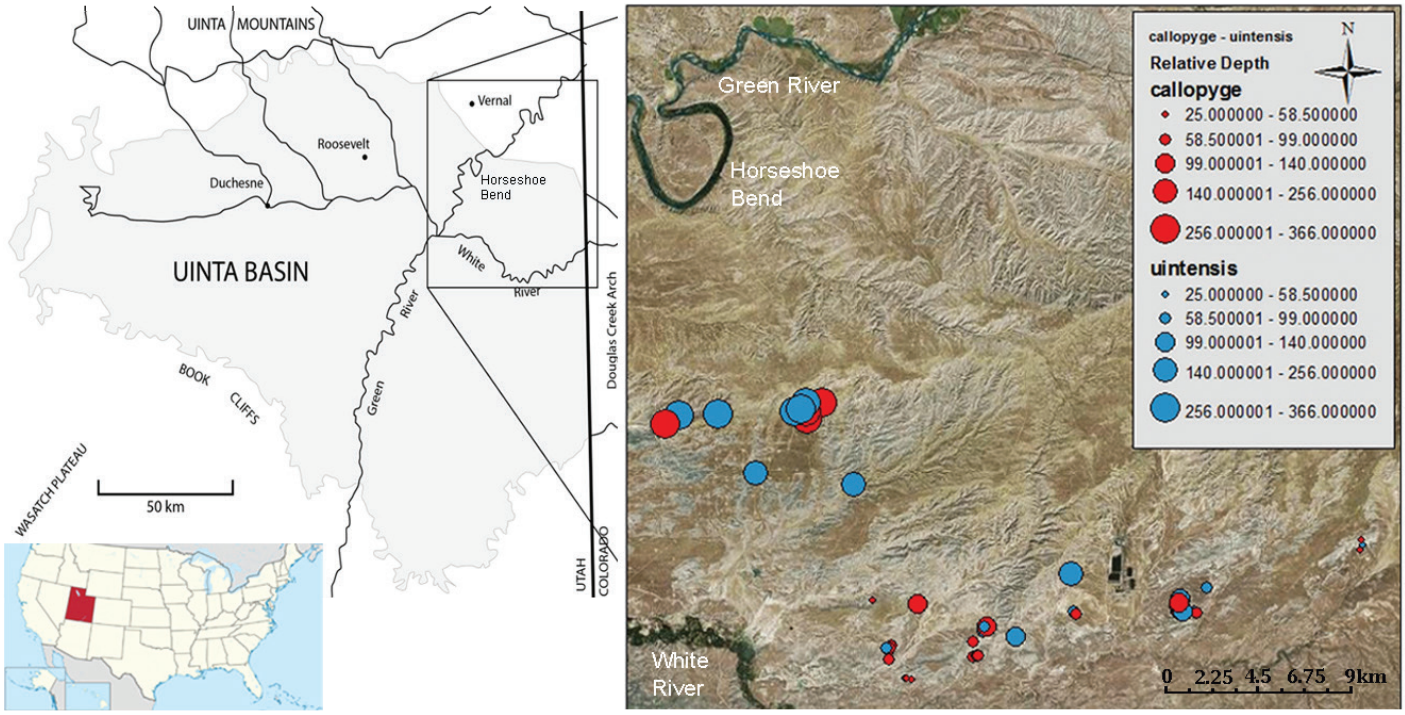

Figure 3. Maps at left showing the location of Utah (inset, Utah shaded red) and the Uinta Basin study site (rectangle). Google map at right showing the spatial relationships of identified Uintan *Echmatemys callopyge* and *E. uintensis* fossil specimens generated in ArcGIS. Symbols represent natural breaks in the data for each species, and are scaled proportional to their stratigraphic meter level. There is no significant difference in the geographic or stratigraphic distributions of these species.

overlap with one or more congeneric species in parts of Honduras and Costa Rica. Pond turtles *Mauremysannamensis* Seibenrock (1903) and *M. sinensis* Gray (1870) may also overlap in parts of China. Additionally, outside of the Geoemydidae, two species of the emydid genus *Terrapene* Merrem, 1820 (box turtles)—*T. carolina* Linneaus, 1758 (common box turtle) and *T. ornata* Agassiz, 1857 (Western box turtle)—show extensive geographic overlap in the central United States.

Morphological Data

Morphological data on epiplastral shape in *Echmatemys* chronospecies were compared using a tiered approach starting with simple linear dimensions, and then progressively to 2D geometric morphometric analyses, and finally to 3D scans. The goal was to assess the comparability of methods and determine whether increased data complexity contributed to greater taxonomic resolution. Results are discussed in order from the simplest to the greatest complexity:

Traditional linear dimensions—Table 3 provides the descriptive statistics for the Tooth-Midline (TM), Tooth-Lip (TL), and TM/TL ratio for each chronospecies (Fig. 1). An ANOVA revealed significant differences among species across the sample (p<0.001) for all three linear variables. However, most pairs of chronospecies did not significantly differ in the TM/TL ratio, suggesting relatively consistent width to length proportions. Only *E. uintensis* and *E.* "Spider Creek" differed significantly from each other (p=0.006), primarily due to the relatively larger TL width compared to TM in *E. uintensis*.

The Regression Analysis revealed a significant correlation between the TM and TL dimensions in the sample (R^2=0.641). A comparison of the correlation between these variables at the intertaxon level indicated different patterns among chronospecies (Fig. 4). In particular, the R^2 values varied from relatively high in *E. uintensis* (R^2=0.672), *E.* "Spider Creek" (R^2=0.632), and *E. septaria* (R^2=0.585) to moderate in *E. haydeni* (R^2=0.199) and *E. testudinea* (R^2=0.444) to low in *E. callopyge* (R^2=0.092). Only the correlation coefficients of *E. callopyge* and *E. uintensis* (z=-1.67, p=0.048) were significantly different from each other, indicating that these two Uintan species exhibit considerably different epiplastral dimensions. A consideration of the type specimens supports this result (Fig. 4), with the *E. uintensis* holotype (AMNH FR 19403) displaying a relatively wider TL distance than the *E. callopyge* holotype (AMNH FR 2807). Each type specimen fell substantially away from the regression line and cluster of the other species.

Table 2. *Echmatemys callopyge* and *E. uintensis* specimens included in the present study, the locality from which they were recovered, and the associated meter level in the stratigraphic section. See Materials and Methods for institutional abbreviations. *Precise meter level not recorded by collectors.

E. callopyge	Locality	Stratigraphic depth (m)
UMNH.VP.26464	L07-08	272
UMNH.VP.26524	WU-18	25
UMNH.VP.26557	WU-26	237
UMNH.VP.26764	WU-210	356
UMNH.VP.26770	WU-50	361
UMNH.VP.27114	WU-8	58.5
UMNH.VP.27220	WU-50	361
UMNH.VP.27443	WU-8	58.5
UMNH.VP.27449	WU-31	95
UMNH.VP.27459	WU-22	87
UMNH.VP.27536	WU-22	87
UMNH.VP.27616	WU-136	140
UMNH.VP.30885	WU-117	123
UMNH.VP.30899	WU-72	98
BYU18833	BYU 42DC379V1	*
UFH-20021715	WU-131	58.5
E. uintensis		
UMNH.VP.26520	WU-6	25
UMNH.VP.26541	WU-8	58.5
UMNH.VP.26558	WU-26	237
UMNH.VP.26746	WU-110	99
UMNH.VP.26765	WU-80A	92
UMNH.VP.26896	WU-129	356
UMNH.VP.27171	WU-129	356
UMNH.VP.27194	WU-8	58.5
UMNH.VP.27397	WU-24	87
UMNH.VP.27429	WU-123	366
UMNH.VP.27432	WU-31	95
UMNH.VP.27573	WU-36	124
UMNH.VP.27621	WU-83	87
UMNH.VP.30895	WU-49	364
UMNH.VP.30498	WU-77	256
UMNH.VP.30560	MWU-16-009	184
UMNH.VP.30803	WU-117	123
BYU18745	Not reported	*
BYU18823	BYU 1383	*
BYU18908	Not reported	Uinta C*
UFH-PR569	Myton Member	Uinta C*

Thus, while significant differences in epiplastral linear dimensions exist between some pairs of *Echmatemys*

chronospecies, not all taxa can be reliably differentiated using these metrics. However, it can be noted that the two Uintan species, *E. callopyge* and *E. uintensis*, differ significantly in their linear epiplastral dimensions.

Two-dimensional landmark data—In the 2D dorsal and ventral PCAs, PC1 and PC2 accounted for a large portion of the total variance: Dorsal=49.3% (PC1) and 16.7% (PC2); Ventral=47.7% (PC1) and 20.8% (PC2). This suggests that 2D geometric morphometric analyses are well-suited to this study. The six *Echmatemys* chronospecies separated to some degree along PC1 and PC2 (Fig. 5). This separation was more pronounced in the dorsal surface analysis, in which *E. uintensis* and *E.* "Spider Creek" fell along the negative side of the PC1 axis, *E. haydeni*, *E. septaria* and *E. testudinea* were positioned in the center, and *E. callopyge* fell along the positive side of the axis (Fig. 5A). A positive PC1 score was associated with a relatively narrower gular scale. In the ventral analysis, there was more apparent overlap among species. The pattern was similar, but all species were clustered more closely together, and *E. septaria* had a wider distribution in both the positive and negative directions (Fig. 5B). The gular scale becomes thinner along the positive direction of PC1, while the gular-humeral sulcus curves more obtusely towards the entoplastron. There was minimal separation along the other PCs in either the dorsal or ventral 2D datasets.

The Procrustes ANOVA results indicated significant differences among the chronospecies. Procrustes ANOVA of dorsal 2D landmarks revealed highly significant differences in shape (F=15.95, p<0.001), and centroid size (F=12.34, p<0.001). For ventral 2D landmarks, significant differences were also revealed among taxa in shape (F=8.20, p<0.001) and centroid size (F=13.33, p<0.001).

Procrustes distances also indicated significant differences between most pairs of taxa in both dorsal and ventral morphology (Table 4). Most notably, the two Uintan *Echmatemys* species were significantly different from each other in both dorsal and ventral epiplastral shape (p<0.001 in both cases) (Table 4). The Bridgerian sample from Spider Creek was highly significantly different from the coeval *E. haydeni* in ventral shape (p<0.001), and significantly different in dorsal shape (p=0.02). However, *E. callopyge* and *E. septaria* did not demonstrate the same level of differentiation in ventral shape (p=0.17) (Table 4). Additionally, the pairwise Procrustes distance between *E. uintensis* and *E. haydeni* (p=0.023) did not reach significance after the correction for multiple tests

Table 3. Descriptive statistics for standard linear measurements of the epiplastron for the six Eocene *Echmatemys* chronospecies included in this study. Please see text and Figure 2 for descriptions. Abbreviations: **PC**=principal component; **SD**=standard deviation; **TM/TL**=tooth to midline/tooth to lip ratio.

Species	Tooth-Midline (TM)		Tooth-Lip (TL)		TM/TL		PC1		PC2	
	Mean	SD	Mean	SD	Mean	SD	Mean	SD	Mean	SD
E. callopyge	4.66	0.78	2.04	0.78	2.56	1.04	-0.051	0.079	0.015	0.037
E. haydeni	3.27	0.59	1.56	0.28	2.11	0.24	-0.022	0.077	-0.009	0.046
E. septaria	2.89	1.14	1.10	0.41	2.70	1.07	-0.049	0.066	-0.001	0.065
E. "Spider Creek"	2.88	0.28	1.55	0.15	1.87	0.20	-0.035	0.055	0.440	0.020
E. testudinea	3.01	0.72	1.38	0.31	2.21	0.47	0.024	0.064	-0.008	0.031
E. uintensis	5.50	0.94	3.25	0.28	1.69	0.18	0.075	0.047	-0.011	0.041
Mean	3.51	1.25	1.65	0.77	2.28	0.81	0.000	0.078	0.000	0.051

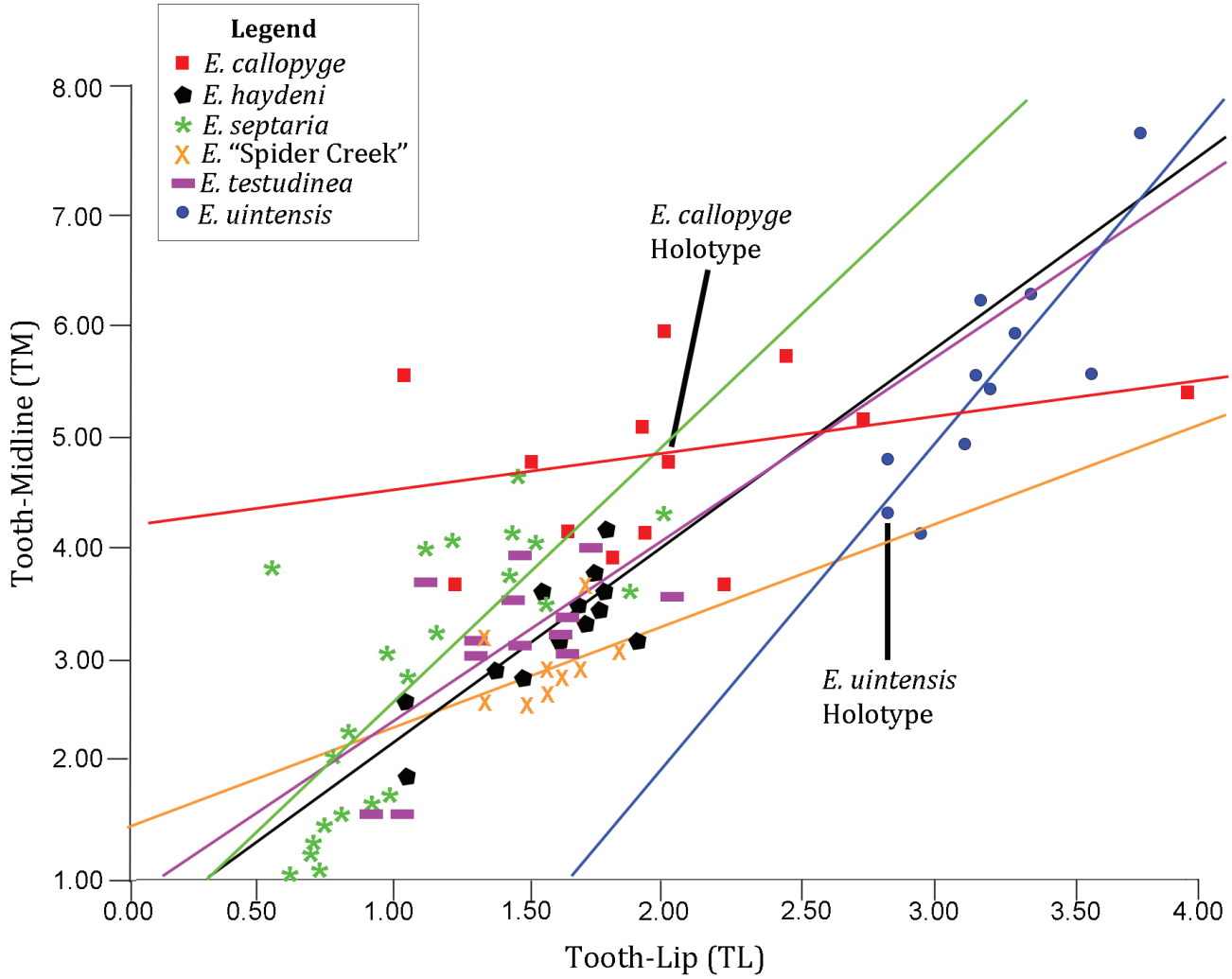

Figure 4. Plot of Tooth-Midline versus Tooth-Lip (TM/TL) values for each specimen. The correlation between these two variables is significant (R^2=0.403). Correlation coefficients do not differ significantly between any pair of taxa.

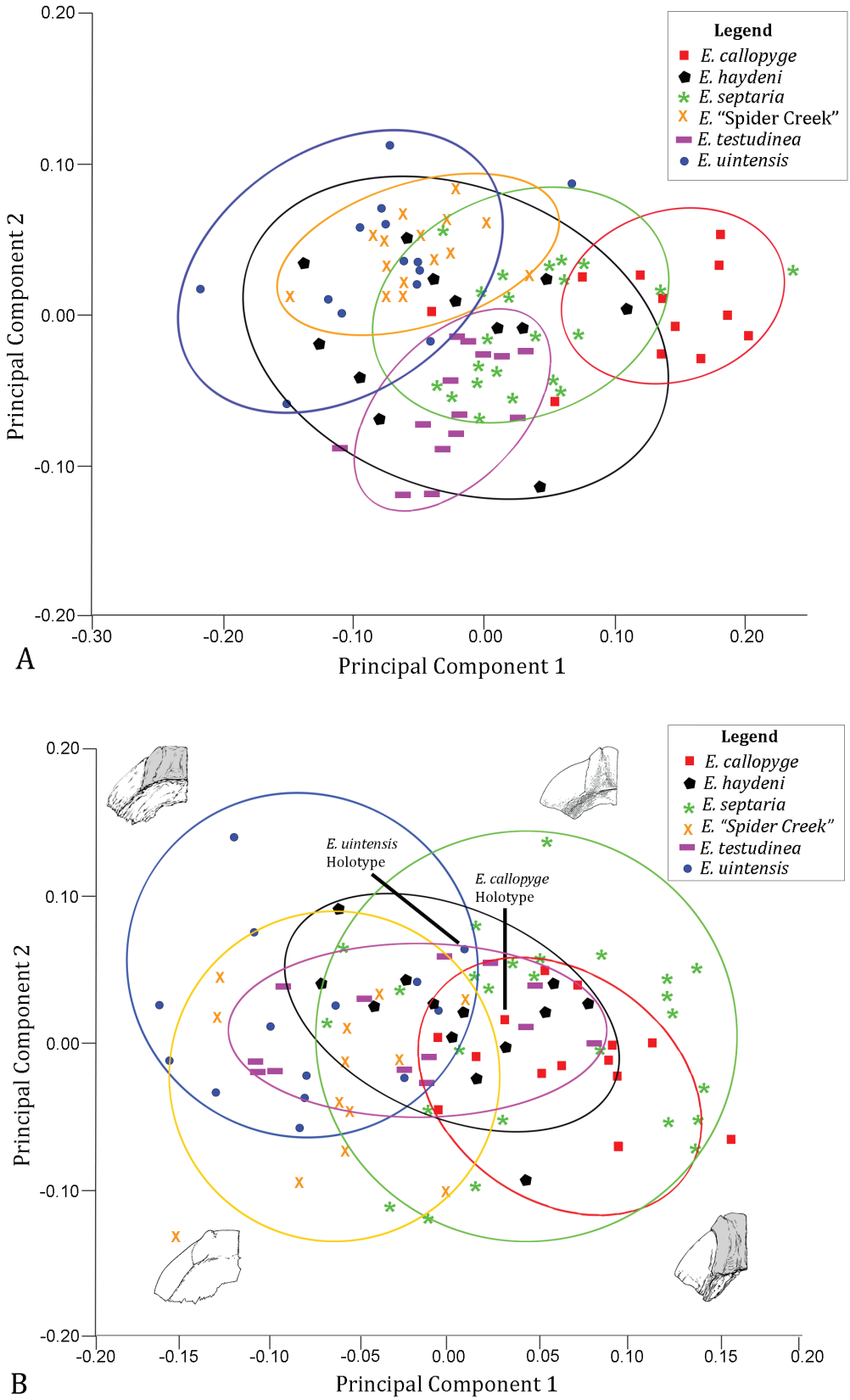

Figure 5. Principal components plots from geometric morphometric analyses of 2D epiplastral shape data. **A**. Dorsal epiplastral shape: PC1 (49.3% variance) versus PC2 (16.7% variance). **B**. Ventral epiplastral shape: PC 1 (47.7% variance) versus PC2 (20.8%) variance.

Table 4. Matrix of pairwise Procrustes distances (*D*) between chronospecies for two-dimensional epiplastral morphology. Procrustes distances for dorsal surface landmarks shaded gray; Procrustes distances for ventral surface landmarks unshaded. Significant pairwise differences (Bonferroni corrected α=0.005) are indicated in bold.

Species	*E. callopyge*	*E. haydeni*	*E. septaria*	*E.* "Spider Creek"	*E. testudinea*	*E. uintensis*
E. callopyge	--	***D*=0.169 *p*<0.0001**	***D*=0.124 *p*<0.0001**	***D*=0.184 *p*<0.004**	***D*=0.184 *p*<0.0001**	***D*=0.232 *p*<0.0001**
E. haydeni	***D*=0.074 *p*=0.002**	--	*D*=0.070 *p*=0.140	*D*=0.063 *p*=0.021	*D*=0.072 *p*=0.015	*D*=0.083 *p*=0.017
E. septaria	*D*=0.044 *p*=0.170	*D*=0.056 *p*=0.035	--	***D*=0.105 *p*<0.001**	***D*=0.108 *p*<0.0001**	***D*=0.132 *p*< 0.0001**
***E.* "Spider Creek"**	***D*=0.140 *p*<0.001**	***D*=0.091 *p*<0.001**	***D*=0.131 *p*<0.001**	--	***D*=0.109 *p*<0.0001**	***D*=0.063 *p*=0.013**
E. testudinea	***D*=0.115 *p*<0.0001**	***D*=0.071 *p*=0.003**	***D*=0.082 *p*=0.002**	***D*=0.097 *p*<0.001**	--	***D*=0.122 *p*<0.0001**
E. uintensis	***D*=0.160 *p*<0.0001**	***D*=0.096 *p*=0.0002**	***D*=0.141 *p*<0.0001**	*D*=0.061 *p*=0.024	***D*=0.085 *p*=0.001**	--

Table 5. Results of three-dimensional epiplastral landmark and semilandmark analyses of *Echmatemys callopyge* and *E. uintensis* in MorphoJ 1.06d. Significant differences between species are highlighted in bold text (Bonferroni corrected α=0.017). CS=centroid size, PC1=principal component 1.

Dataset	Sample Size	Procrustes ANOVA: Shape	Procrustes ANOVA: CS	Regression: PC1 vs CS	Procrustes distance
Full epiplastron	37	***F*=16.24 *p*<0.001**	*F*=1.43 *p*=0.2402	*R*=0.282 *p*=0.090	***D*=0.223 *p*<0.001**
Dorsal surface	37	***F*=3.25 *p*<0.001**	*F*=2.63 *p*=0.114	*R*=0.280 *p*=0.093	***D*=0.037 *p*=0.011**
Ventral surface	37	***F*=3.32 *p*<0.001**	*F*=0.56 *p*=0.460	*R*=0.106 *p*=0.532	***D*=0.042 *p*=0.012**

Figure 6. Principal components plots from geometric morphometric analyses of 3D epiplastral shape. **A**. Full epiplastron (dorsal and ventral surfaces) (PC1=69.4% variance, PC2=12.6%). **B**. Dorsal epiplastral shape (PC1=38.6%, PC2=27.0%).

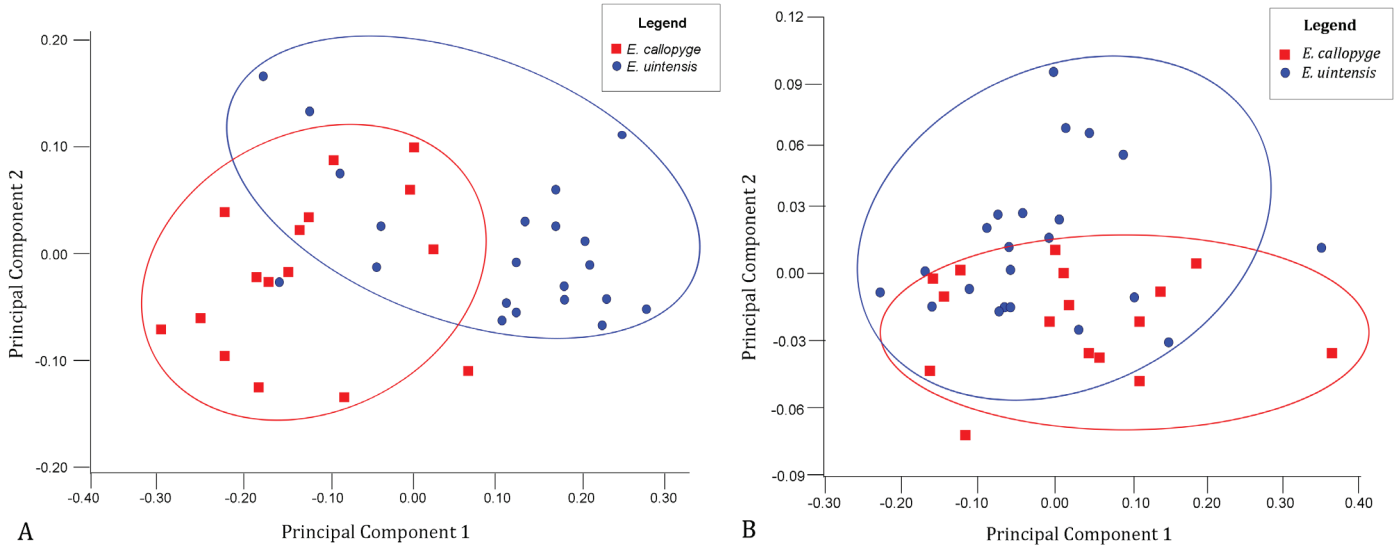

Figure 6 (cont.). Principal components plots from geometric morphometric analyses of 3D epiplastral shape. **C**. Ventral epiplastral shape (PC1=38.6%, PC2=27.0%). Significant differences were revealed in 3D shape of the epiplastron for all three comparisons: Full epiplastron (p<0.001), dorsal surface (p=0.011), and ventral surface (p=0.012).

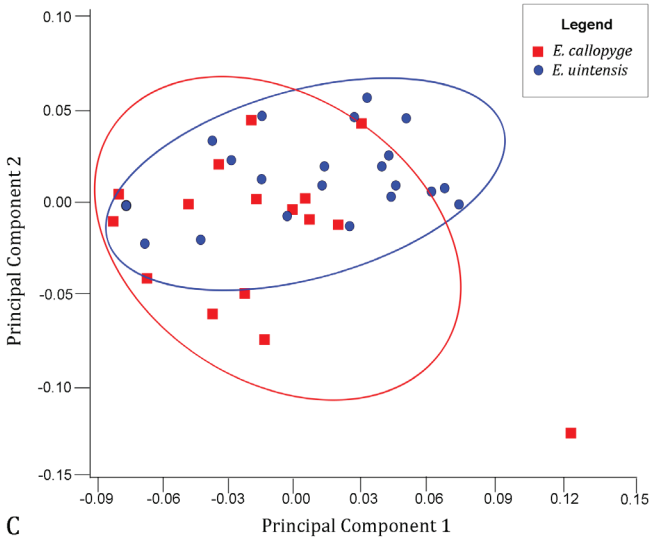

was applied (Bonferroni α=0.005).

In the ventral 2D dataset, the ANOVA revealed

significant differences among taxa for PC1 (p<0.001) and PC3 (p<0.001). Tukey pairwise tests found significant differences between most pairs of taxa in PC1. For dorsal 2D morphology, the ANOVA revealed significant interspecific differences for PCs 1 through 3 (p<0.001 in all cases). Tukey post hoc tests indicated significant differences between many pairs of taxa for PC1. Most notably, *E. callopyge* + *E. uintensis* were again revealed to be significantly different (p<0.001), as were *E. haydeni* and *E.* "Spider Creek" (p=0.022). A comparison of the positions of the holotypes of *E. callopyge* and *E. uintensis* (Fig. 5B) indicates that these type specimens diverge along PC2, while their PC1 scores are more similar.

A Regression Analysis between PC1 scores and the TM/TL ratio revealed a significant but moderate correlation between these variables across the sample (R^2=0.403). The highest correlations were found in *E. testudinea* (R^2=0.711) and *E. uintensis* (R^2=0.578), while the relationship was lower in *E. septaria* (R^2=0.320), *E. haydeni* (R^2=0.293), and *E. callopyge* (R^2=0.252). None of these species-level correlations differed significantly from each other.

Three-dimensional landmark data—The PCAs for all three 3D datasets—the full epiplastron, and dorsal and ventral surfaces—indicated a clear separation between *E. callopyge* and *E. uintensis* along PC1 (Table 5; Fig. 6). In the full epiplastral 3D analysis, a higher PC1 score was associated with a dorsal sulcus that was more laterally oriented, while a lower score was associated with a more caudally oriented dorsal sulcus relative to the ventral sulcus (Fig. 6A). In the dorsal and ventral epiplastral 3D datasets, the separation was less marked than in the full epiplastral dataset (Fig. 6B, C). The warp analysis indicated that to warp *E. callopyge* into *E. uintensis* required increasing both the overall width of the gular scale and its angle (Fig. 7). It also required extending the epiplastral tooth anteriorly, indicating that the average *E. uintensis* has a more projecting tooth than *E. callopyge* (Fig. 7).

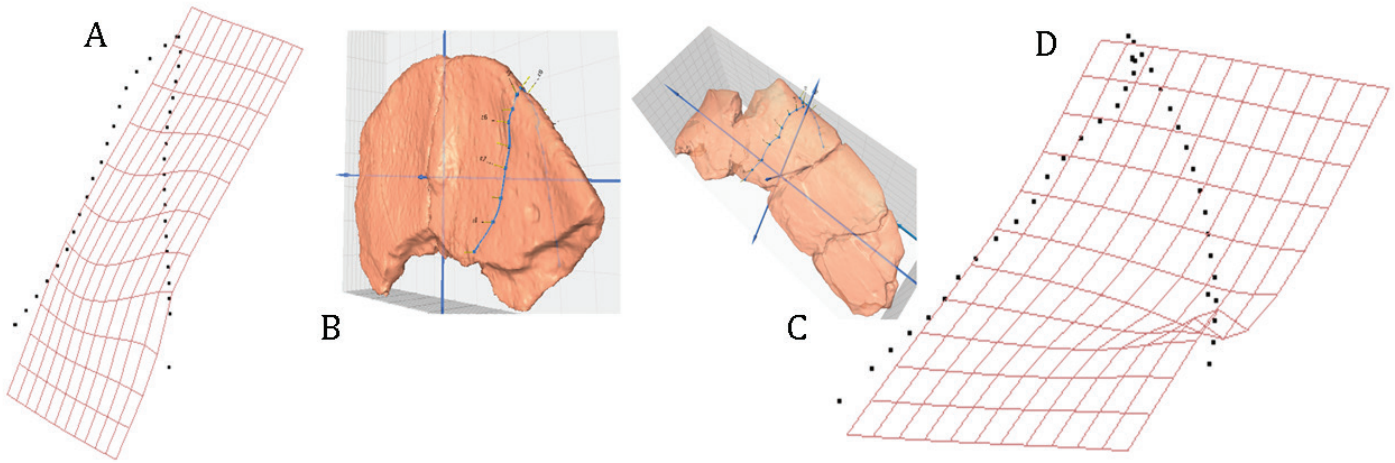

Figure 7. Results of sliding semilandmark process from 3D data, and specimens warped along Principal Component 1 (PC1). **A.** Thin plate spline deformation grid showing transformation of *Echmatemys callopyge* mean type along PC1. **B**. 3D image of *Echmatemys callopyge* showing the positions of landmarks along the curve indicated in **A**, specimen no.UNMN.VP.27621. **C**. 3D image of *Echmatemys uintensis* showing the positions of landmarks along the curve indicated in D, UMNH.VP.27429. **D**. Thin plate spline deformation grid showing transformation of *E. uintensis* mean type along PC1.

The Procrustes ANOVA revealed highly significant differences between species in the shape of the epiplastron for each of the 3D datasets, $p<0.001$ in all three cases (Table 5). However, no significant interspecific differences were noted in centroid size (Table 5). These analyses indicate that *E. callopyge* and *E. uintensis* are significantly different in the three-dimensional shape of the epiplastron.

DISCUSSION

Geographic Distribution

The two Uintan *Echmatemys* species, *E. callopyge* and *E. uintensis*, exhibit extensive geospatial and stratigraphic overlap across the study site and throughout the section (e.g., Townsend et al. 2006, 2010). The extensive geographic overlap between species highlights the need for accurate methods of taxonomic identification, such as epiplastral shape analyses described here, because provenance alone cannot be used to differentiate between *E. callopyge* and *E. uintensis*.

The fact that two large-bodied, congeneric river turtle species would occupy the same geographic distribution might initially seem surprising; however, our comparison of extant geoemydids indicates that this is not an uncommon phenomenon in this family. A similar pattern has also been documented among extant marine turtles (e.g., Pate and Salmon 2017). In the study site in the Uinta Basin, *Echmatemys* is also frequently found in association with other aquatic and semi-aquatic turtles, including baenids (an extinct family of large-bodied river turtles), trionychids (soft-shelled turtles), and carettochelyids (pig-nosed turtles). Future studies could evaluate the particular local environments shared by *E. callopyge* and *E. uintensis* in the context of Uinta Basin herpetofaunal communities, which are poorly understood compared to mammals. The areas from which these Uintan turtles were recovered include large river channels and deltaic sands prograding into Lake Uinta as it regressed westward (Bryant et al. 1989, Davis et al. 2008, Smith et al. 2008).

Epiplastral Shape

The linear, 2D-landmark, and 3D-landmark epiplastral morphological results all demonstrate that Uintan *E. callopyge* and *E. uintensis* can be reliably differentiated using the shape of the epiplastron and gular scale. In particular, the 3D shape of the epiplastron appears to be a particularly valuable interspecific indicator (Table 3; Fig. 6). In addition, significant separation between these taxa was also obtained using both the linear and 2D epiplastral datasets. These results strongly support previous observations (Hay 1908, Gilmore 1915, Roberts 1962, Hutchison 2002) pertaining to the comparative narrowness of *E. callopyge* epiplastra. This study also confirms that the shape of the gular scale differs significantly between these two Uintan taxa, and can distinguish the two species.

Despite the significant difference in epiplastral shape between *E. callopyge* and *E. uintensis* in all analyses, many other included *Echmatemys* species did not separate out using this character. In the linear analyses, *E. septaria* differed significantly from *E. uintensis* and *E. haydeni*, but all other pairs of taxa overlapped. This suggests that simple epiplastral linear dimensions and ratios do not have the power to reliably differentiate between *Echmatemys* species outside of *E. uintensis* and *E. callopyge*. In the 2D landmark analyses, most pairs differed significantly, except *E. callopyge* and *E. septaria* (ventral). *E. uintensis* and *E. haydeni* (dorsal) also failed to achieve significance after the correction for multiple comparison was applied ($p=0.023$). These findings may indicate that these taxa have an ancestor-descendant relationship, since *E. haydeni* dates to earlier horizons. However, *E. haydeni* exhibits some unique characteristics of the carapace, including a heterogeneous neural series (Vlachos 2017), not currently reported in *E. callopyge*, although this feature has not been fully evaluated in the latter.

It has been suggested that the genus *Echmatemys* is in need of comprehensive taxonomic revision (Vlachos 2017). While *Echmatemys* appears to be monophyletic in most phylogenetic analyses, its species generally form an unresolved polytomy (e.g., Vlachos 2017, Vlachos and Rabi 2017). The number of species within *Echmatemys* has been the subject of extensive debate, and is beyond the scope of this paper. However, the finding that epiplastral shape can differentiate among *Echmatemys* chronospecies may contribute to future revisions of the genus, and improved accuracy of such techniques can assist in future evaluations. The overlap between Uintan *E. callopyge* and Bridgerian *E. septaria* in both linear (Fig. 4) and ventral 2D morphology (Fig. 5B) is notable given that some researchers have suggested that these taxa may actually represent the same species (Gilmore 1915, Roberts 1962). In 1962, Roberts redefined *E. callopyge* as a subspecies of *E. septaria* based on a shared narrow epiplastral shape. While the present study does not specifically address this question, it is worth noting that these allotaxa are significantly different in dorsal ($p<0.001$) but not ventral 2D epiplastral morphology.

Thus, the overall shape of the epiplastron is similar between them, but the ventral outline of its gular scale

is not. Additionally, the specimens from Spider Creek separate out from contemporaneous Bridgerian samples attributed to *E. haydeni* in several datasets, suggesting that the Spider Creek material may represent a new undescribed species. Unfortunately, the holotypes of *E. haydeni* and *E. septaria* do not include complete epiplastra, so they are not available for direct comparison using the current methods.

Methodology

This hierarchical comparison of methodologies also provides insight into the relative necessity of the more logistically complicated, time-consuming laser scans versus simple photographs. The 3D scans provided the greatest differentiation among species. The 2D landmark-based comparisons were also reliable for distinguishing between the two Uintan species. However, the linear comparisons primarily differentiated between only the Uintan species and did not reliably differentiate among *Echmatemys* species from other NALMAs.

There are considerable logistical advantages to the types of 2D data evaluated here. Both linear dimensions and 2D landmark data can be accurately obtained from photographs, which means that such data can be collected quickly in the field, at museums, or from published or shared photographs (as discussed in Schneider et al. 2012). Collecting two-dimensional data can also allow researchers to maximize their limited museum time. For example, in the amount of time it takes to 3D scan a single specimen, dozens of photographs could be taken. As discussed above, 2D landmark-based analyses provide a high level of separation among all *Echmatemys* species evaluated here. Future studies attempting to use epiplastral shape to differentiate along taxa should weigh whether the time and computational effort required for 3D scans and analyses is worth the additional resolution beyond the 2D information available from photographs.

ACKNOWLEDGEMENTS

Funding for this research was provided by Midwestern University faculty intramural funds (to HFS and KET). We thank Dr. Patricia Holroyd (UCMP), Dr. Rodney Scheetz (BYU), and Dr. Steve Sroka (UFH) for access to fossil material in their care. We thank Kelsey Jorge for assistance scanning many of the Uinta Basin specimens included in this study, and Avery Williams for assistance with fossil curation. Specimens from the Uinta Basin were collected under permits issued by the Bureau of Land Management to KET, and we appreciatively acknowledge their cooperation. We also acknowledge the assistance of the Uinta Basin field crew over numerous field seasons, including Dr. Penny Higgins, Dr. Pat Holroyd, Karen McCormick, Dr. Laura Stroik, Jeffrey Westgate, and Dr. Jim Westgate. We thank C. Levitt-Bussian and J. Krishna (UMNH) for assistance in curation. The authors wish to thank Peter Kloess (Associate *PaleoBios* editor) and two anonymous reviewers for their constructive comments that strengthened the paper.

LITERATURE CITED

Adrian, B., Smith, H.F., Noto, C.R., and A. Grossman. 2019. A new baenid, "*Trinitichelys*" *maini* sp. nov., and other fossil turtles from the Upper Cretaceous Arlington Archosaur Site (Woodbine Formation, Cenomanian), Texas, U.S.A. *Palaeontologia Electronica* 22.3.80:1–29.

Agassiz, L.R. 1857. Contributions to the natural history of the United States of America. Little, Brown and Company, London. 452 pp.

Anquetin, J., Puntener, C., and W.G. Joyce. 2017. A review of the fossil record of the clade *Thalassochelydia*. *Bulletin of the Peabody Museum of Natural History* 58:317–369.

Baur, G. 1891. Notes on some little known American fossil tortoises. *Proceedings of the Academy of Natural Sciences of Philadelphia* 43:411–430.

Brinkman, D.B. 2003. Anatomy and systematics of *Plesiobaena antiqua* (Testudines: Baenidae) from the mid-Campanian Judith River Group of Alberta, Canada. *Journal of Vertebrate Paleontology* 23:146–155.

Bryant, B., C.W. Naeser, R.F. Marfin, and H.H. Mehnert. 1989. Upper Cretaceous and Paleogene sedimentary rocks and isotopic ages of Paleogene tuffs, Uinta Basin, Utah. *USGS Bulletin* 1989:1787-J.

Cope, E.D. 1873a. On the extinct Vertebrata of the Eocene of Wyoming observed by the Expedition of 1872, with notes on the geology. In F.V. Hayden (ed.), *Sixth Annual Report of the United States Geological Survey of the Territories,* pp545–649.

Cope, E.D. 1873b. Descriptions of some new Vertebrata from the Bridger Group of the Eocene. *Proceedings of the American Philosophical Society* 12:460–465.

Cope, E.D. 1876. On some extinct reptiles and Batrachia from the Judith River and Fox Hills Beds of Montana. *Proceedings of the Academy of Natural Sciences of Philadelphia* 28:340–359.

Daudin, F. 1801. Histoire Naturelle, Generale et particuliere, des Reptiles, Vol. 1. F. Dufart, Paris, 432 pp.

Davis, S.J., B.A. Wiegand, A.R. Carroll, and C.P. Chamberlain. 2008. The effect of drainage reorganization on paleoaltimetry studies: An example from the Paleogene Laramide foreland. *Earth Planet Science Letters* 275:258–268.

Dryden, I.L., and K.V. Mardia. 1998. Statistical shape analysis. Wiley, London. 347 pp. Duméril, A.M., G. Bibron, and A. Duméril. 1851. Catalogue methodique de la collection des reptiles du Museum d'Histoire Naturelle. Gide and Boudry, Paris. 224 pp.

Duméril, A.M., G. Bibron, and A. Duméril. 1851. Catalogue methodique de la collection des reptiles du Museum d'Histoire Naturelle. Gide and Boudry, Paris. 224 pp.

ESRI. 2011. ArcGIS Desktop: Release 10. Environmental Systems Research Institute, Redlands, CA.

Fitzinger L. 1835. Entwurf einer systematischen Anordnung der Schildkröten nach den Grundsätzen der natürlichen Methode. *Annalen des Wiener Museums der Naturgeschichte* 1:105–128.

Gaffney E.S., H. Tong, and P.A. Meylan. 2006. Evolution of the side-necked turtles: the families Bothremydidae, Euraxemydidae, and Araripemydidae. *Bulletin of the American Museum of Natural History* 300:1–318.

Gilmore, C.W. 1915. The fossil turtles of the Uinta Formation. *Memoirs of the Carnegie Museum* 7:101–161.

Goodall, C.R. 1991. Procrustes methods and the statistical analysis of shape (with discussion). *Proceedings of the Royal Society of London B Biological Sciences* 53:285–340.

Gower, J.C. 1975. Generalised procrustes analysis. *Psychometrika* 40:33–50.

Gray, J.E. 1825. A synopsis of the genera of reptiles and amphibia, with a description of some new species. *Annals of Philosophy* 10:193–217.

Gray, J.E. 1831. *Synopsis Reptilium; or short descriptions of the species of reptiles, Part I. Cataphracta. Tortoises, crocodiles, and enaliosaurians*. Treutel, Wurtz, and Co., London.

Gray, J.E. 1856. Catalogue of shield reptiles in the collection of the British Museum. Part I. Testudinata (Tortoises). British Museum, London. 79 pp.

Gray, J.E. 1860. Description of new species of *Geoclemmys* from Ecuador. *Proceedings of the Zoological Society of London* 1860:231–232.

Gray, J.E. 1870. Supplement to the catalogue of shield reptiles in the collection of the British Museum. Part 1. Testudinata (Tortoises). Taylor and Francis, London. 120 pp.

Gunnell, G.F., P.C. Murphey, R.K. Stucky, K.E. Townsend, P. Robinson, J.-P. Zonneveld, and W. Bartels. 2009. Biostratigraphy and biochronology of the latest Wasatchian, Bridgerian, and Uintan North American Land Mammal "Ages". *Museum of Northern Arizona Bulletin* 65:279–330.

Hay, O.P. 1906. Descriptions of two new genera (*Echmatemys* and *Xenochelys*) and two new species (*Xenochelys formosa* and *Terrapene putnami*) of fossil turtles. *Bulletin of the American Museum of Natural History* 22:27–31.

Hay, O.P. 1908. The fossil turtles of North America. *Carnegie Institution of Washington Publication* no. 75.

Hutchison, J.H. 2002. Guide to the turtles of the Uinta Formation. Unpublished field guide.

Hutchison, J.H. 2006. *Bridgeremys* (Geoemydidae, Testudines), a new genus from the middle Eocene of North America. Pp. 63–83 *in* I.G. Danilov and J.F. Parham (eds.). Fossil Turtle Research, Vol.1.

IBM Corp. Released 2013. SPSS Statistics for Windows, version 22. Armonk, NY: IBM Corp.

Jenks, G.F. 1967. The data model concept in statistical mapping. *International Yearbook of Cartography* 7:186–190.

Joyce, W.G. 2016. A review of the fossil record of turtles of the clade Pan-Chelydridae. *Bulletin of the Peabody Museum of Natural History* 57:21–56.

Joyce, W.G. 2017. A review of the fossil record of basal Mesozoic turtles. *Bulletin of the Peabody Museum of Natural History* 58:65–113.

Joyce, W.G, and T.L. Lyson. 2015. A review of the fossil record of turtles in the clade Baenidae. Bull *Peabody Museum of Natural History* 56(2):147–183.

Joyce, W.G., J.F. Partham, and J.A. Gauthier. 2004. Developing a protocol for the conversion of rank-based taxon names to phylogenetically defined clade names, as exemplified by turtles. *Journal of Paleontology* 78:989–1013.

Joyce, W.G., F.A. Jenkins, and T. Rowe. 2006. The presence of cleithra in the basal turtle *Kayentachelys aprix*; pp. 93–103 in I. G.Danilov, and J. F. Parham (eds.), *Fossil Turtle Research*. *Russian Journal of Herpetology 13* (Suppl. 1). Zoological Institute of Russian Academy of Sciences, St. Petersburg.

Klingenberg, C.P. 2011. MorphoJ: an integrated software package for geometric morphometrics. *Molecular Ecology Resources* 11:353–357.

Linneaus, C. 1758. Systema naturæ per regna tria naturæ, secundum classes, ordines, genera, species, cum characteribus, differentiis, synonymis, locis. Tomus I. Salvius, Stockholm. 824 pp.

Lyson, T.L., and W.G. Joyce. 2010. A new Baenid turtle from the Upper Cretaceous (Maastrichian) Hell Creek Formation of North Dakota and a preliminary taxonomic review of Cretaceous Baenidae. *Journal of Vertebrate Paleontology* 30:394–402.

Merrem, B. 1820. Tentamen systematic amphibiorum. Krieger, Marburg. 191 pp.

O'Higgins, P., and N. Jones. 2006. Tools for statistical shape analysis. Hull York Medical School. [http://sites.google.com/site/hymsfme/resources.]

Pate, J.H., and M. Salmon. 2017. Ontogenetic niches and the development of body shape in juvenile sea turtles. Chelonian Conservation and Biology 16:185–193.

Prothero, D.R. 1996. Magnetic stratigraphy and biostratigraphy of the middle Eocene Uinta Formation, Uinta Basin, Utah. Pp. 4–23 *in* D.R. Prothero and R.J. Emry (eds.). The Terrestrial Eocene-Oligocene Transition in North America. Cambridge University Press, Cambridge, Massachusetts.

Roberts, D.C. 1962. A study of *Echmatemys callopyge* from the Uinta Eocene of Utah, and its redefinition as a subspecies of *E. septaria*. *Bulletin of the Museum of Comparative Zoology* 127:375–399.

Rohlf, F.J. 2006. tpsDig. State University of New York, Department of Ecology and Evolution, Stony Brook, NY.

Schneider, C.A., W.S. Rasband, and K.W. Eliceiri. 2012. NIH Image to ImageJ: 25 years of image analysis. *Nature Methods* 9:671–675.
Siebenrock, F. 1903. Schildkroten des ostlichen Hinterindien. *Sitzungsberichte der Kaiserlichen Akademie der Wissenschaften in Wien (Mathemathisch-Naturwissenschaftliche Klasse)* 112(1):333–353.

Siebenrock, F. 1903. Schildkroten des ostlichen Hinterindien. *Sitzungsberichte der Kaiserlichen Akademie der Wissenschaften in Wien (Mathemathisch-Naturwissenschaftliche Klasse)* 112(1):333-353.

Smith, M.E., A.R. Carroll, and B.S. Singer. 2008. Synoptic reconstruction of a major ancient lake system: Eocene Green River Formation, western United States. *Geological Society of America Bulletin* 120:54–84.

Townsend, K.E., A.R. Friscia, and D.T. Rasmussen. 2006. Stratigraphic distribution of upper Middle Eocene vertebrate localities in the eastern Uinta Basin, Utah, with comment on Uintan biostratigraphy. *Mountain Geology* 43:115–134.

Townsend, K.E., D.T. Rasmussen, P.C. Murphey, and E. Evanoff. 2010. Middle Eocene habitat shifts in the North American western interior: A case study. *Palaeogeography, Palaeoclimatology, Palaeoecology* 297:144–158.

Vitek, N.S., and W. G. Joyce. 2015. A review of the fossil record of New World turtles of the clade. Pan-Trionychidae. *Bulletin of the Peabody Museum of Natural History* 56:185–244.

Vlachos E. 2017. A review of the fossil record of the clade Pan-Testudinoidea. Bulletin of the *Peabody Museum of Natural History* 59:3–94.

Vlachos E., and M. Rabi. 2017. Total evidence analysis and body size evolution of extant and extinct tortoises (Testudines: Cryptodira: Pan-Testudinidae). *Cladistics* 34:652–683.